A complete energy transfer map for COF2

J. L. Ahl, R. K. Bohn, K. H. Casleton, Y. V. C. Rao, and George W. Flynn

Citation: The Journal of Chemical Physics **78**, 3899 (1983); doi: 10.1063/1.445113
View online: http://dx.doi.org/10.1063/1.445113
View Table of Contents: http://scitation.aip.org/content/aip/journal/jcp/78/6?ver=pdfcov
Published by the AIP Publishing

A complete energy transfer map for COF_2 [a)b)]

J. L. Ahl, R. K. Bohn, K. H. Casleton, Y. V. C. Rao, and G. W. Flynn

Department of Chemistry and Columbia Radiation Laboratory, Columbia University, New York, New York 10027

(Received 15 July 1982; accepted 15 September 1982)

Fluorescence from the ν_1, ν_4, ν_6, and ν_3/ν_5 states has been observed following Q-switched CO_2 laser excitation of the ν_2 C–F stretch mode of COF_2. A kinetic model is presented which is consistent with the observed fluorescence lifetimes. Following excitation of the ν_2 mode, $2\nu_2$ is rapidly pumped by ladder climbing collisions. The $2\nu_2$ states are collisionlessly coupled to the ν_1 mode by Fermi resonance leading to the creation of a steady state between the ν_1 and ν_2 manifolds within 30 gas kinetic collisions. Subsequently, the ν_2 state decays to the ν_6 mode in 800 collisions, and also fills the ν_4 mode in 2000 gas kinetic collisions. The ν_4 level rapidly equilibrates with the near resonant states $2\nu_3$, $2\nu_5$, and $\nu_3+\nu_5$ after about 25 collisions, and these states rapidly decay to the ν_3 and ν_5 fundamentals in less than or about 100 collisions. The ν_6 state relaxes to the ν_3/ν_5 states, in approximately 190 collisions, while vibration-translation/rotation relaxation of ν_3 and ν_5 to the ground state occurs on a time scale of 1200 collisions.

INTRODUCTION

The study of vibrational energy transfer processes in simple polyatomic molecules can contribute to an enhanced understanding of molecular interactions. While there have been many studies of vibrational relaxation mechanisms, most of these investigations provide information only on the macroscopic relaxation of the emitting states rather than on the more useful microscopic kinetic rate processes. The kinetic rate constants can be determined only if the paths for vibrational relaxation are known unambiguously.[1,2]

The molecule COF_2 is a particularly convenient species in which to study intermode energy transfer as all of the vibrational modes are infrared active.[3–5] In addition, COF_2 differs from most of the other polyatomic molecules which have been investigated as it is composed entirely of heavy atoms. As a result, most of the vibrational modes are relatively low frequency leading to a relatively dense vibrational manifold at low energies (see Fig. 1). The large moments of inertia should reduce the effects of the rotational degrees of freedom on vibrational energy transfer, and as a result, COF_2 should serve as an approximate model for the energy transfer properties of larger molecules.

Two prior studies,[3,4] which focused on the relaxation of the ν_1 and the ν_4 states, have allowed a partial mapping of the energy transfer processes in COF_2. By observing the laser induced fluorescence emission from each of the fundamental states following CO_2 laser excitation of the ν_2 C–F symmetric stretch mode, we have been able to determine the complete energy transfer map for COF_2, including both the major pathways for vibrational energy transfer in the molecule, and the kinetic rate constants for these processes.

EXPERIMENTAL

The experimental apparatus used in these laser induced fluorescence studies consisted of a Q-switched CO_2 laser operating on either the $P(20)$ or the $R(22)$ 10.6 μ lines. The laser produced 2 mJ pulses at a repetition rate of 200 hz, with a pulse width, measured at the 5% points of less than 1 μs.

Laser induced fluorescence signals from the COF_2 ν_1, ν_4, ν_6, and the (ν_3, ν_5) states were observed at right angles to the pump laser. As the emission from these states covers a large wavelength range, several in-

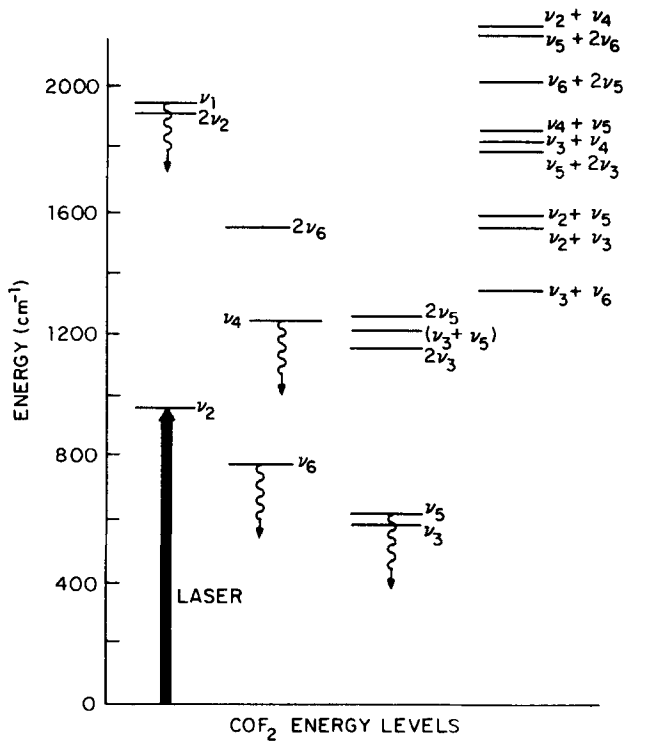

FIG. 1. The energy level diagram for COF_2 according to the data of Ref. 5. The pulsed CO_2 laser excitation is marked with a heavy arrow and the observed fluorescence are shown by wavy arrows.

[a)]Work supported by the National Science Foundation under Grant CHE-80-23747 and the Joint Services Electronics Program (U.S. Army, U. S. Navy, and U. S. Air Force) of the Department of Defense under Contract No. DAAG29-79-C-0079. Equipment support provided by the Department of Energy under Contract DE-AC02-78ER04940.

[b)]Present addresses: J. K. Ahl, Science Applications, Inc., McLean, Virginia; R. K. Bohn, Department of Chemistry, University of Connecticut, Storrs, Connecticut; K. H. Casleton, Morgantown Energy Technology Center, Morgantown, W. Virginia; Y. V. C. Rao, Department of Chemical Engineering, Indian Institute of Technology, Kanpur, India.

TABLE I. Experimental fluorescence growth and decay rates and amplitude ratios for COF_2.

Wavelength	State	Rates[a]				Amplitude ratio
5 μ	ν_1	7.6 ± 0.8[d]	30 ± 3[d]		545 ± 50[e]	$I_{30}/I_8 = 5.5$[b]
8 μ	ν_4	7.0 ± 1[d]	28.6 ± 3[e]	155 ± 20[e]		$I_{155}/I_{30} = 0.94$[c]
13 μ	ν_6	8.0 ± 1[d]	96 ± 7[e]			
16 μ	$\nu_{3,5}$	8 ± 1[d]	30 ± 3[e]			

[a]Rates are experimentally determined rate of growth or decay, expressed in units of $ms^{-1}\,Torr^{-1}$.
[b]Ratio of 5 μ fast decay amplitude to slow decay amplitude.
[c]Ratio of 8 μ fast rise amplitude to slow rise amplitude.
[d]Rate occurs in the decay of the fluorescence.
[e]Rate occurs in the rise of the fluorescence.

frared detectors were used.

The short wavelength emission from ν_1, at 5 μ, was observed with a photo-voltaic InSb detector (cutoff wavelength 5.5 μ) viewing the fluorescence region through a 4.6 μ long pass filter. The laser was attenuated to approximately 200 μJ when studying ν_1 to avoid nonlinearities in the kinetic pathways. The emission from the ν_4 mode, at 8 μ, was isolated by a 7.5 to 8.5 μ bandpass filter and a MgF_2 window, and detected by a AuGe detector. The ν_6 state at 13 μ was viewed through three stacked 11.4 μ long pass filters and was detected by a "type c" material HgCdTe detector with a cutoff wavelength at 15 μ. The lowest energy states ν_3 and ν_5 are too close to separate with interference filters. A 16 μ long pass filter and a CuGe detector were used to observe fluorescence from this pair of states.

The 5, 8, and 16 μ fluorescences were observed with the CO_2 laser operating on the $P(20)$ 10.6 μ line. To reduce the effects of laser scatter, the 13 μ emission was observed with the laser tuned to the $R(22)$ 10.6 μ line. Fluorescence from the 13 μ state following excitation with the laser tuned to $P(20)$ was otherwise identical to the fluorescence following $R(22)$ excitation.

Each of the detectors was equipped with a wideband matched preamplifier and exhibited risetimes of between 1 and 2 μs, including the laser pulse width. The fluorescence signals were averaged by a Biomation 8100 transient digitizer/Nicolet 1174 combination, and stored on a lab computer for later analysis.

The COF_2 sample was obtained from Synthatron Corp. and used without further purification. Infrared spectra of the COF_2 taken in stainless steel absorption cells showed the samples to be essentially free from CO_2 and other contaminants. The CO_2 impurity referred to in an earlier study, resulted from the reaction of the COF_2 with a glass IR absorption cell.[4] A sample of COF_2 left in a glass cell for 24 h was observed to decompose entirely into SiF_4 and CO_2 products. In the current study, the only materials in contact with the gas were the stainless steel cell walls, viton o rings and the NaCl or KBr fluorescence windows. The stainless steel fluorescence cell had an outgas rate of < 10 mTorr h^{-1}.

RESULTS

Time dependent fluorescence from the ν_1, ν_4, ν_6, and ν_3/ν_5 states has been observed as a function of COF_2 pressure. All of the fluorescence curves exhibit an exponential rise and then decay back to a thermal tail level. The thermal tail,[6] created as a result of increased black body radiation due to gas heating by the exothermic $V-V$ and $V-T$ relaxation processes, slowly decays to the baseline. The slowly decaying thermal tail was fit to a single exponential functional form by a least squares fitting program. The calculated curve was then subtracted from the original data, and the process repeated to extract both the decay rates and the amplitudes for a given fluorescence. These rates were plotted vs total pressure and the averaged eigenvalues determined from the slopes of the curves.

Each state has a characteristic set of eigenvalues and amplitudes (Table I), however, a few eigenvalues appear in several states.

5 μ fluorescence

The ν_1 state fluorescence exhibits a single exponential rise followed by a double exponential decay. The measured eigenvalues are 545 ± 50 $ms^{-1}\,Torr^{-1}$ for the rise, 30 ± 3 $ms^{-1}\,Torr^{-1}$ for the fast decay, and 7.6 ± 0.8 $ms^{-1}\,Torr^{-1}$ for the slow decay. The amplitude of the fast decay was approximately five times the slow decay amplitude. The errors are quoted as ± 3 sigma. These results are consistent with the earlier work of Casleton and Flynn.[3]

8 μ fluorescence

The 8 μ fluorescence from ν_4 is composed of a double exponential rise and a single exponential decay. The fast rise eigenvalue was 155 ± 20 $ms^{-1}\,Torr^{-1}$, the slow rise eigenvalue was 28.6 ± 3 $ms^{-1}\,Torr^{-1}$, and the decay eigenvalue was measured to be 7.0 ± 1 $ms^{-1}\,Torr^{-1}$ in agreement with the work of Bohn *et al.*[4] The amplitudes of the two rise times were approximately equal.

13 μ fluorescence

The ν_6 state fluorescence consists of a single exponential rise followed by a single exponential decay. The rate of rise is 96 ± 7 $ms^{-1}\,Torr^{-1}$ and the rate of decay is 8.0 ± 1 $ms^{-1}\,Torr^{-1}$.

16 μ fluorescence

Fluorescence from the pair of states ν_3 and ν_5 was observed at 16 μ. The signals exhibit a single expo-

nential rise and a single exponential decay. The rise eigenvalue was 30 ± 3 $ms^{-1}\,Torr^{-1}$ and the decay eigenvalue was 8 ± 1 $ms^{-1}\,Torr^{-1}$.

There are a total of ten exponential terms in the fluorescences of the four emitting states, however, it appears that there are only five unique eigenvalues. The smallest eigenvalue 8 $ms^{-1}\,Torr^{-1}$, appears in the fluorescence of each state. The 30 $ms^{-1}\,Torr^{-1}$ eigenvalue appears in three of the states ν_1, ν_3/ν_5, and ν_4.

KINETICS

An examination of the qualitative features of the eigenvalues and eigenvectors of the COF_2 fundamental bands (Table I) provides a great deal of information about the detailed kinetic mechanism involved in the intermode equilibration process. While earlier studies focused on the behavior of the individual states ν_1 and ν_4, we now have information on the behavior of all of the low lying states of the molecule and can suggest a plausible mechanism for the relaxation of vibrational energy in COF_2.

The smallest eigenvalue 8 $ms^{-1}\,Torr^{-1}$ occurs in the fluorescence of each mode. This suggests that the system has already reached $V-V$ equilibrium and this eigenvalue is associated with the $V-T/R$ relaxation of the molecule as a whole. This relaxation is most likely through the lowest exothermic pathway

$$COF_2(\nu_3) + COF_2 \xrightarrow{k'_{VT}} COF_2(\nu_0) + COF_2 + 582\ cm^{-1}\ , \qquad (1)$$

$$COF_2(\nu_5) + COF_2 \xrightarrow{k''_{VT}} COF_2(\nu_0) + COF_2 + 619\ cm^{-1}\ . \qquad (2)$$

The largest eigenvalue 545 $ms^{-1}\,Torr^{-1}$ appears only in the rise of the fluorescence of the ν_1 state. Casleton and Flynn[3] have attributed this eigenvalue to the combination of the ladder climbing mechanism

$$COF_2(\nu_2) + COF_2(\nu_2) \rightarrow COF_2(2\nu_2) + COF_2(0) + 14\ cm^{-1}$$

and the rapid transfer of population between the $2\nu_2$ state and the ν_1 state due to the strong Fermi mixing of the two levels. Therefore, the states ν_2 and ν_1 equilibrate rapidly and the slower eigenvalues in the 5 μ emission represent the decay of population out of the ν_2 states, as well as out of the ν_1 and $2\nu_2$ states. Since the population of the ν_2 state is approximately 150 times larger than that of ν_1 or $2\nu_2$, the decay of the coupled states is almost certainly dominated by relaxation of ν_2 to the closest lying fundamentals ν_4 and ν_6:

$$COF_2(\nu_2) + COF_2 \xrightarrow{k_{24}} COF_2(\nu_4) + COF_2 - 280\ cm^{-1}\ , \qquad (3)$$

$$COF_2(\nu_2) + COF_2 \xrightarrow{k_{26}} COF_2(\nu_6) + COF_2 + 188\ cm^{-1}\ . \qquad (4)$$

Thus, the remaining eigenvalue in the 5 μ fluorescence 30 $ms^{-1}\,Torr^{-1}$ will represent the decay of energy out of ν_2 and therefore we have the *approximate* relationship: $k_{24} + k_{26} = 30$ $ms^{-1}\,Torr^{-1}$.

The 8 μ fluorescence from the ν_4 state displays the 30 $ms^{-1}\,Torr^{-1}$ eigenvalue consistent with the state being pumped from ν_2. This state also exhibits a fast eigenvalue occurring in the fluorescence rise (155 $ms^{-1}\,Torr^{-1}$). Bohn *et al.*[4] have proposed a limited three level model consisting of the states ν_2, ν_4, and the tightly coupled set of states $2\nu_3$, $2\nu_5$, and $(\nu_3+\nu_5)$, where the kinetic pathways consist of reaction (3) and the additional reactions

$$COF_2(\nu_4) + COF_2 \xrightarrow{k'_{4x}} COF_2(2\nu_3) + COF_2 + 78\ cm^{-1}\ , \qquad (5)$$

$$COF_2(\nu_4) + COF_2 \xrightarrow{k''_{4x}} COF_2(2\nu_5) + COF_2 + 4\ cm^{-1}\ , \qquad (6)$$

$$COF_2(\nu_4) + COF_2 \xrightarrow{k'''_{4x}} COF_2(\nu_3+\nu_5) + COF_2 + 41\ cm^{-1}\ . \qquad (7)$$

As noted earlier,[4] because of the relatively balanced coupling of the different modes, the kinetic rate constants calculated with the three level system are in substantial disagreement with the rate constants calculated below using a more complete six level model; however the suggested mechanism in which ν_4 is emptied faster than it fills appears to be a necessary part of any kinetic model. The major consequence of this reversal of more "normal" kinetic behavior is that one of the rates (eigenvalues) appearing in the *fluorescence rise* actually corresponds to a physical process which empties the state (ν_4) being observed. Furthermore, a slower kinetic rate (eigenvalue), appearing in the fluorescence at a *later time* (slow rise of ν_4), actually corresponds to the physical process which fills the state. While this behavior seems intuitively strange, it is by no means unprecedented and provides a strong manifestation of the difficulties encountered in unraveling coupled kinetic equations. This phenomenon has been discussed elsewhere in detail for COF_2.[4]

The overtone states $2\nu_3$, $2\nu_5$, and $(\nu_3+\nu_5)$ will relax by a reverse ladder climbing mechanism to the fundamentals

$$COF_2(2\nu_3) + COF_2 \xrightarrow{k'_d} COF_2(\nu_3) + COF_2(\nu_3)\ , \qquad (8)$$

$$COF_2(2\nu_5) + COF_2 \xrightarrow{k''_d} COF_2(\nu_5) + COF_2(\nu_5)\ , \qquad (9)$$

$$COF_2(\nu_3+\nu_5) + COF_2 \xrightarrow{k'''_d} COF_2(\nu_3) + COF_2(\nu_5)\ . \qquad (10)$$

These events (8)–(10) can be expected to reach steady state in less than or about 100 collisions.

The 13 μ fluorescence from the ν_6 state exhibits only a single eigenvalue (96 $ms^{-1}\,Torr^{-1}$), besides the $V-T$ rate. We attribute this eigenvalue to the $V-V$ decay of ν_6 to the states ν_3 and ν_5:

$$COF_2(\nu_6) + COF_2 \xrightarrow{k'_{63}} COF_2(\nu_3) + COF_2 + 192\ cm^{-1}\ , \qquad (11)$$

$$COF_2(\nu_6) + COF_2 \xrightarrow{k''_{63}} COF_2(\nu_5) + COF_2 + 155\ cm^{-1}\ . \qquad (12)$$

The equations (1)–(12) complete our proposed model for the kinetics of vibrational energy transfer between the modes of COF_2. The rate equations can be simplified by assuming that the nearly resonant states ν_3 and ν_5 are tightly coupled. This pair of states will be labeled ν_3. Similarly, the three near resonant overtone states $2\nu_3$, $2\nu_5$, and $\nu_3+\nu_5$ are rapidly equilibrated and are represented as ν_x. As above, the rate constant for the transfer of population from state i to state j is k_{ij} and the reverse rate is k_{ji}. The $V-T,R$ relaxation rate for ν_3 is k_{VT} and the reverse rate for this process

is k_{TV}. The ladder climbing processes from ν_3 to ν_x is given by k_u while the down-the-ladder rate is k_d. These rates are for the microscopic processes and the degeneracy of the states has been explicitly included in the rate equations rather than in the rate constants.

The resulting bimolecular kinetic rate equations are

$$\dot{N}_4 = -(k_{42}+k_{4x})NN_4 + k_{24}NN_2 + k_{x4}NN_x ,$$

$$\dot{N}_x = -k_{x4}NN_x - k_d N_0 N_x + k_{4x}NN_4 + k_u N_3 N_3 ,$$

$$\dot{N}_3 = -k_{36}NN_3 - 2k_u N_3 N_3 - k_{VT}NN_3 + k_{63}NN_6 + 2k_d N_0 N_x + k_{TV}NN_0 ,$$

$$\dot{N}_6 = -(k_{62}+k_{63})NN_6 + k_{26}NN_2 + k_{36}NN_3 ,$$

$$\dot{N}_0 = -(k_d N_x + k_{TV}N)N_0 + k_u N_3 N_3 + k_{VT}NN_3 ,$$

$$\dot{N}_2 = -(k_{24}+k_{26})NN_2 + k_{42}NN_4 + k_{62}NN_6 ,$$

where the total number of molecules in all levels is N, the population in the pair of states ν_3 and ν_5 is N_3, and the total population of the states $2\nu_3$, $2\nu_5$, and $(\nu_3+\nu_5)$ is N_x.

The population of a given level N_i can be expanded as a sum of the equilibrium population N_i^0 plus a deviation term $n_i(t)$: $N_i = N_i^0 + n_i(t)$. After substituting these expressions into the rate equations, terms in $N_i^0 \times N_j^0$ can be eliminated because the equilibrium conditions make their sum equal to zero. Terms of the order of $n_i \times n_j$ are neglected as they are small compared with terms of the form $N_i^0 \times n_j$ for the low level excitation conditions of these experiments.[6,7]

The constraint equation for the conservation of total particles

$$n_4 + n_x + n_3 + n_6 + n_0 + n_2 = 0$$

can be applied to reduce the original six equation system to only five equations. Applying the detailed balance conditions: $k_{42} = 3.84k_{24}$, $k_{4x} = 3.65k_{x4}$, $k_u = 0.75k_d$, $k_{TV} = 0.112k_{VT}$, $k_{63} = 4.62k_{36}$, $k_{62} = 0.405k_{26}$, we arrive at the final set of coupled differential equations written in matrix form (where the factor N, the total population density, has been suppressed from each matrix entry)

$$\begin{bmatrix} \dot{n}_4 \\ \dot{n}_x \\ \dot{n}_3 \\ \dot{n}_6 \\ \dot{n}_0 \end{bmatrix} = \begin{bmatrix} -(k_{4x}+4.84k_{24}) & (k_{x4}-k_{24}) & -k_{24} & -k_{24} & -k_{24} \\ 3.65k_{x4} & -(k_{x4}+0.859k_d) & 0.1436k_d & 0 & -0.00801k_d \\ 0 & 1.718k_d & -(k_{36}+0.288k_d+k_{VT}) & 4.62k_{36} & (0.016k_d+0.112k_{VT}) \\ -k_{26} & -k_{26} & (k_{36}-k_{26}) & -(1.405k_{26}+4.62k_{36}) & -k_{26} \\ 0 & -0.859k_d & (0.1436k_d+k_{VT}) & 0 & -(0.00801k_d+0.112k_{VT}) \end{bmatrix} \times \begin{bmatrix} n_4 \\ n_x \\ n_3 \\ n_6 \\ n_0 \end{bmatrix}$$

The roots of this rate matrix are the eigenvalues observed in the fluorescence traces. Given the eigenvalues, it is not possible to determine the rate constants of the system analytically. Instead, a computer program calculates both the eigenvalues and eigenvectors for a given set of guessed rate constants. These rate constants were adjusted to generate a best fit to the observed eigenvalues and amplitude ratios.

The best fit rate constants are listed in Table II, and the eigenvalues and amplitude ratios calculated using these rate constants are shown in Table III. The calculated values are in good agreement with the observed data. The mathematical description for the time dependent populations of ν_4, $\nu_{3,5}$, ν_6, and ν_2 are as follows:

$$n_4/n = -0.006e^{-937t} - 0.016e^{-159t} + 0.013e^{-94t} - 0.039e^{-30t} + 0.048e^{-8t} ,$$

$$n_{3,5}/n = -0.002e^{-937t} + 0.188e^{-159t} + 0.115e^{-94t} - 1.087e^{-30t} + 0.887e^{-8t} ,$$

$$n_6/n = 0e^{-973t} - 0.052e^{-159t} - 0.1128e^{-94t} - 0.053e^{-30t} + 0.233e^{-8t} ,$$

$$n_2/n = 0e^{-973t} + 0.007e^{-159t} + 0.009e^{-94t} + 0.816e^{-30t} + 0.168e^{-8t} .$$

TABLE II. Experimentally derived energy transfer rate constants and probabilities for COF_2.

Transition		Rate constant (ms^{-1} $Torr^{-1}$)	Probability[a]
$\nu_2 \rightarrow \nu_4$	(k_{24})	8 ± 3	4.96×10^{-4}
$\nu_2 \rightarrow \nu_6$	(k_{26})	20 ± 5	1.24×10^{-3}
$\nu_6 \rightarrow \nu_{3,5}$	(k_{63})	83 ± 20	5.20×10^{-3}
$2\nu_3$			
$\nu_4 \rightarrow \nu_3+\nu_5$	(k_{4x})	700 ± 200	4.35×10^{-2}
$2\nu_5$			
$2\nu_3$ $2COF_2(\nu_3)$			
$\nu_3+\nu_5 \rightarrow COF_2(\nu_3)+COF_2(\nu_5)$	(k_d)	$140+210/-40$	9.44×10^{-3}
$2\nu_5$ $2COF_2(\nu_5)$			
$\nu_3, \nu_5 \rightarrow \nu_0$	(k_{VT})	13 ± 2	8.13×10^{-4}
$(2\nu_2, \nu_1) \rightarrow 2COF_2(\nu_2)$		550 ± 30	3.3×10^{-2}

[a]A collision diameter of 6 A and a temperature of 296 K were used to convert energy transfer rates to probabilities. The probability is defined as $k/k_{\text{gas-kinetic}}$.

TABLE III. Calculated fluorescence eigenvalues (ms^{-1} $Torr^{-1}$) and amplitude ratios for COF_2.

Wavelength	State	Calculated eigenvalues[a]			Amplitude ratio
5 μ	$\nu_1(\nu_2)$	8	30		$I_{30}/I_8 = 4.9$
8 μ	ν_4	8	30	159	$I_{159}/I_{30} = 0.41$
13 μ	ν_6	8	94		
16 μ	$\nu_{3,5}$	8	30		

[a]Eigenvalues calculated with the derived rate constants. $k_{24}=8$, $k_{26}=20$, $k_{x4}=190$, $k_d=140$, $k_{63}=83$, $k_{VT}=13$ (units are ms^{-1} $Torr^{-1}$).

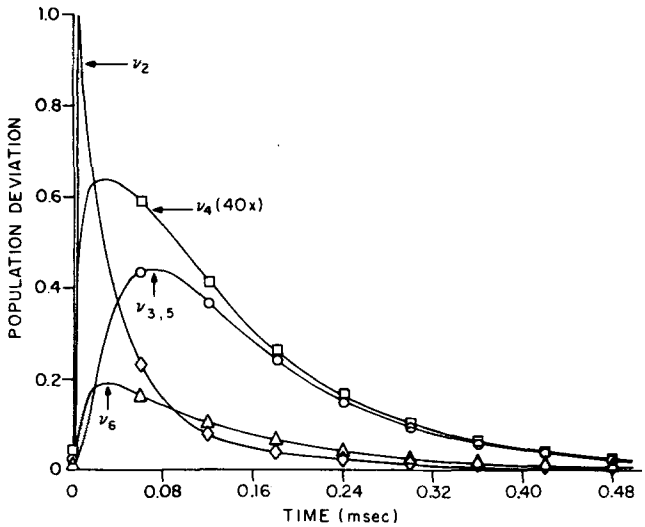

FIG. 2. The calculated time evolution of the vibrational populations of the COF_2 fundamental levels. Thermal heating effects and the slow thermal decay have been neglected. These curves were calculated using Eqs. (1)–(12) and the experimentally derived rate constants $k_{24}=8$, $k_{26}=20$, $k_{x4}=190$, $k_d=140$, $k_{63}=83$, $k_{VT}=13$ (units are $ms^{-1}Torr^{-1}$). The pressure was taken to be 1 Torr.

Here n is the number of molecule/cm^3 originally excited to ν_2, t is in ms, and a pressure of 1 Torr has been assumed. A plot of the population deviations is shown in Fig. 2.

While the ν_1 and $2\nu_2$ states have not been included in this model, they are not expected to significantly affect the above results as they are tightly coupled to the ν_2 fundamental and their steady state populations are less than 1% of the ν_2 population. A more serious problem is the presence of a thermal tail in the raw data. While the eigenvalues can be accurately extracted from the data, the amplitude ratios include the effects of the thermal tail. A complete analytical solution should include the effects of heat transport,[8,9] however we expect that thermal relaxation will not significantly alter the calculated rate constants.

Since the eigenvalue and amplitude spectrum of the kinetic rate matrix cannot be uniquely inverted to obtain kinetic rate constants[7] (especially with the present state of experimental art which provides only a limited number of eigenvalues and amplitudes of what is in reality a very large rate matrix), the present computer fitting procedures in some cases produce kinetic rate constants with considerable error. Nevertheless, based on the sensitivity of the experimental data to the chosen rate constants, some comments can be made about the reliability of the rate constants deduced by this procedure and given in Table II. In particular, the ladder climbing rate for filling ν_1, $2\nu_2$ is almost completely decoupled from the relaxation of the remainder of the modes and hence yields an accurate rate constant within the approximation that these two states can be treated as a single level.[3] The overall fast decay of ν_2 (observed through ν_1, $2\nu_2$ fluorescence) can be measured with high accuracy because of the excellent signal quality of the ν_1, $2\nu_2$, fluorescence. This leads to a very reliable value for the sum $k_{24}+k_{26}$ which corresponds closely to the 30 $ms^{-1}Torr^{-1}$ eigenvalue. The breakup of this sum into individual contributions attributable to k_{24} and k_{26} is noticeably less certain. The rate constant k_{63} is reasonably accurate though the relatively poor signal quality for ν_6 fluorescence plus interference from the rate constant k_{26} (which feeds ν_6) leads to some uncertainty. The rate constant k_d corresponding to deactivation of the levels $2\nu_3$, $2\nu_5$, $\nu_3+\nu_5$ is the least certain because the eigenvalue for this process could not be directly observed at all. Rather, k_d's value was set by determining its effect on the predicted fluorescence from ν_4. The rate constant k_{4x} can also be determined only with low accuracy because its value depends significantly on k_d. k_{4x} and k_d couple in their effect on ν_4 fluorescence though k_{4x} contributes more directly to the rate and shape of this signal. Finally, the $V-T$ rate constant k_{VT} can be determined with relatively high accuracy since it is closely related to the slowest observed eigenvalue of the kinetic rate matrix (8 $ms^{-1}Torr^{-1}$); however, because this eigenvalue also has contributions (~ 25%) from the intermode kinetic rate constants, k_{VT} is less well determined than is normally the case for small polyatomic molecules. The error limits listed in Table II for all rate constants reflect at least qualitatively the considerations noted above.

DISCUSSION

Theoretical predictions using a short-range repulsive interaction model

The probability that a polyatomic molecule will change its vibrational quantum state during a collision can be calculated using SSH theory,[10] modified to include the breathing sphere approximation.[11,12] SSH theory calculates the energy transfer probability assuming a one-dimensional collision, using a purely repulsive, exponential potential and harmonic wave functions. The theory does not include the effects of long range attractive forces or the influence of rotations.

The SSH probability is given by

$$P_{i,f}=P_0(a)\,P_0(b)\,g_f|U_{i,f}|^2 I(\Delta E, T, \mu, L, \epsilon)\ ,$$

where $P_0(a)$ and $P_0(b)$ are steric factors equal to 2/3 for a nonlinear molecule; g_f is the degeneracy of the final state; $|U_{i,f}|^2$ is the vibrational matrix element for the transition. The translational factor I is a function of the energy gap of the transition (ΔE), the translational temperature (T), the reduced mass of the colliders (μ), the repulsive interaction length (L), and the Lennard-Jones well depth (ϵ).

Vibrational energy transfer probabilities for COF_2 have been calculated using a Lennard-Jones well depth parameter ϵ/k of 111.9 K,[13] and an exponential range parameter L equal to 0.2 A. Varying the range parameter L between 0.15 and 0.25 A did not qualitatively alter the results.

The breathing sphere amplitudes A_j^2 for each of the normal vibrations of COF_2 were determined following the method of Stretton.[11] The transformation matrix

B, relating the internal coordinates to the Cartesian displacement coordinates, was obtained by the method of Wilson, Decius, and Cross.[14] The symmetry coordinates, molecular geometry, and the transformation matrix L^{-1} for the molecule COF_2 were taken from Mallinson *et al.*[5] The calculated breathing sphere parameters are: $A^2_{\nu_1}=0.0071$, $A^2_{\nu_2}=0.017$, $A^2_{\nu_3}=0.016$, $A^2_{\nu_4}=0.0044$, $A^2_{\nu_5}=0.0178$, and $A^2_{\nu_6}=0.0101$ amu^{-1}.

The vibrational matrix elements were calculated using harmonic wave functions[15] and are listed in Table IV.

The calculated and experimentally determined probabilities and collision numbers (Z) for COF_2 are shown in Table V. The energy gaps and probabilities for the three single quantum exchange processes $\nu_4 \rightarrow \nu_2$ ($\Delta E = 280$ cm^{-1}, $Z_{expt}=525$), $\nu_2 \rightarrow \nu_6$ ($\Delta E = 188$ cm^{-1}, $Z_{expt}=800$), and $\nu_6 \rightarrow \nu_{3,5}$ ($\Delta E = 192/155$ cm^{-1}, $Z_{expt}=192$) are approximately equal. Apparently, energy is transferred between an in-plane vibration (ν_2 or $\nu_{3,5}$) and an out-of-plane vibration (ν_6) as efficiently as between two in-plane vibrations. The SSH probabilities are significantly smaller than the experimental results for these deactivation processes, yet the theory correctly predicts that the processes $\nu_2 \rightarrow \nu_6$ and $\nu_6 \rightarrow \nu_{3,5}$ will occur at approximately the same rate.

The calculated probability for the $\nu_4 \rightarrow \nu_2$ process is predicted to be significantly slower than the $\nu_2 \rightarrow \nu_6$ and $\nu_6 \rightarrow \nu_{3,5}$ processes. This difference is due to both the larger energy gap for this event, which results in a smaller translational factor I, and also, to the small breathing sphere amplitude of the ν_4 state. The experimental probabilities for this transition are clearly larger than those calculated by the simple theory. This may be due to the anharmonicity of the ν_4 state induced by the mixing of ν_4 with the near resonant set of states $2\nu_3$, $2\nu_5$, and $\nu_3+\nu_5$. This could enhance the vibrational matrix element for the state ν_4, since the modes ν_3 and ν_5 have a larger breathing sphere amplitude.

Further evidence for this mixing can be found in a comparison of the experimental and theoretical probabilities for the processes $\nu_4 \rightarrow 2\nu_3$, $2\nu_5$, and $\nu_3+\nu_5$. The experimental probability ($Z=23$) is three orders of magnitude larger than the SSH probability. The large observed probabilities and the small energy gaps for these processes strongly suggest the presence of either a symmetry allowed Fermi resonance mixing of the ν_4 and $\nu_3+\nu_5$ states, with an energy gap of 41 cm^{-1}, or a Coriolis coupling of ν_4 with any of these three states.

TABLE IV. Vibrational matrix elements $|U_{if}|^2$ for COF_2.[a]

Transition	$\lvert U_{i,f}\rvert^2$
$\nu_2 \rightarrow \nu_4$	1.1×10^{-5}
$\nu_2 \rightarrow \nu_6$	4.1×10^{-5}
$\nu_6 \rightarrow \nu_3, \nu_5$	6.6×10^{-5}
$\nu_4 \rightarrow 2\nu_3$	1.09×10^{-7}
$\nu_4 \rightarrow \nu_3+\nu_5$	2.19×10^{-7}
$\nu_4 \rightarrow 2\nu_5$	1.11×10^{-7}
$\nu_3, \nu_5 \rightarrow \nu_0$	1.2×10^{-2}

[a]Calculated assuming harmonic oscillator wave functions, and a repulsive range parameter L equal to 0.2 A.

TABLE V. Experimental and theoretical energy transfer probabilities and collision numbers for COF_2.

		Probability		Collision number[a]	
Transition	ΔE[b]	SSH[c,d]	Exptl.	SSH	Exptl
$\nu_2 \rightarrow \nu_4$	−280	1.0×10^{-6}	4.96×10^{-4}	988 000	2000
$\nu_4 \rightarrow \nu_2$	+280	3.9×10^{-6}	1.92×10^{-3}	257 000	525
$\nu_2 \rightarrow \nu_6$	188	8.9×10^{-5}	1.24×10^{-3}	11 400	800
$\nu_6 \rightarrow \nu_3$	192	1.3×10^{-4}	5.20×10^{-3}	7 760	192
$\nu_6 \rightarrow \nu_5$	155	2.8×10^{-4}	5.20×10^{-3}	3 640	192
$\nu_4 \rightarrow 2\nu_3$	78	1.9×10^{-6}		722 000	
$\nu_4 \rightarrow \nu_3+\nu_5$	41	6.9×10^{-6}	4.35×10^{-2}	145 000	23
$\nu_4 \rightarrow 2\nu_5$	4	4.6×10^{-6}		215 000	
$\nu_3 \rightarrow \nu_0$	582	1.7×10^{-5}	8.13×10^{-4}	52 000	1230
$\nu_5 \rightarrow \nu_0$	619	8.9×10^{-6}		111 000	

[a]Collision numbers are the reciprocals of probabilities.
[b]A positive ΔE denotes an exothermic process.
[c]Energy transfer probabilities were calculated using the "SSH-breathing sphere" model, assuming harmonic oscillator wave functions.
[d]Probabilities are calculated assuming a collision diameter of 6 A and a temperature of 296 K.

The theoretical probabilities for the V–T,R processes $\nu_{3,5} \rightarrow \nu_0$ are approximately a factor of 30 smaller than the experimental results. This behavior is typical of SSH calculations for the V–T relaxation of most polyatomic molecules. Frequently, this poor agreement arises from the presence of H atoms in the molecule which leads to high rotational velocity around at least one principal axis. This in turn can provide an alternate vibration-rotation (V–R) relaxation mechanism not included in the SSH formalism. For COF_2, which is composed of all heavy atoms, such a mechanism is not realistic. The poor agreement for COF_2 may simply indicate that the potential surface for two colliding COF_2 molecules is too complex to be modeled as a completely spherical, exponentially repulsive process. Alternatively, a still different mechanism, such as the mixing of a few rotational levels in different vibrational states due to anharmonic forces,[6,21] may be active.

Comparison of the energy transfer probabilities for COF_2, SO_2, CO_2, OCS, and N_2O

Partial vibrational energy transfer maps are known for four, nonhydrogen containing, polyatomics other than COF_2: the linear molecules OCS, CO_2, and N_2O and the nearly symmetric top SO_2. A comparison of the energy transfer rates in these molecules can provide a qualitative test for energy transfer theories. The vibration to translation/rotation energy transfer probabilities for the five molecules are listed in Table VI. With regard to the V–T/R relaxation efficiencies, the two nonlinear molecules COF_2 and SO_2 stand out as anomalies compared to the linear set of OCS, N_2O, and CO_2. Thus, even though all five molecules in Table VI have about the same energy gap, the linear ones clearly relax more slowly. It is perhaps worth noting that a

TABLE VI. Probability of vibrational-translational/rotational energy transfer for COF_2, OCS, SO_2, N_2O, and CO_2.

Species	ΔE[b]	Collision number[a]
$COF_2(\nu_{3,5} \rightarrow \nu_0)$	582/619	1230[c]
SO_2 $(\nu_2 \rightarrow \nu_0)$	518	700[d]
$OCS(\nu_2 \rightarrow \nu_0)$	520	4600[e]
N_2O $(\nu_2 \rightarrow \nu_0)$	589	10 000[f]
CO_2 $(\nu_2 \rightarrow \nu_0)$	667	46 000[g]

[a]Collision numbers are the reciprocals of probabilities.
[b]A positive ΔE (cm^{-1}) denotes an exothermic process.
[c]This work.
[d]See Refs. 16 and 17.
[e]See Ref. 1 and 18.
[f]See Ref. 19.
[g]See Refs. 19 and 20.

mechanism in which crossover from the lowest vibrational level of a molecule into the ground state proceeds via mixing of a small number of rotational states by either anharmonic or Coriolis coupling[6,21] would be favored in the nonlinear systems due to their relatively high density of rotational states.

In the case of $V-V$ transfer for the all heavy atom species shown in Table VII, the most remarkable feature is the similarity of the energy transfer efficiencies for systems with energy gaps in the 150–280 cm^{-1} range where only the exchange of a single quantum of vibrational energy for each mode is involved. Thus, all the COF_2 entries and the $SO_2(\nu_1 \rightarrow \nu_3)$ process have collision numbers covering the relatively narrow range 175–700 collisions. For processes which involve energy transfer from an overtone level to a fundamental, considerable variability exists in the energy transfer probabilities. This is not surprising since such processes are expected to be extremely sensitive functions of the anharmonic mixing between the overtone and the fundamental.[1,6,30]

CONCLUSIONS

Vibrational energy transfer processes in COF_2 have been studied using a laser induced fluorescence technique and the dominant energy transfer pathways determined. Upon excitation of the ν_2 mode, the following sequence of events (summarized in Fig. 3) occurs:

(1) The ν_2 state rapidly equilibrates with the $2\nu_2$ state (in about 30 gas kinetic collisions) by a near resonant ladder climbing mechanism. The ν_1 state is also pumped by this process due to the strong Fermi mixing of the ν_1 and $2\nu_2$ states. (A collision diameter of 6 A and a temperature of 296 K were used to convert energy transfer rates to probabilities.)

(2) The ν_2 state decays via two competitive processes. (a) The ν_4 state is pumped by the endothermic reaction

$$COF_2(\nu_2) + COF_2 \rightarrow COF_2(\nu_4) + COF_2 - 280\ cm^{-1}$$

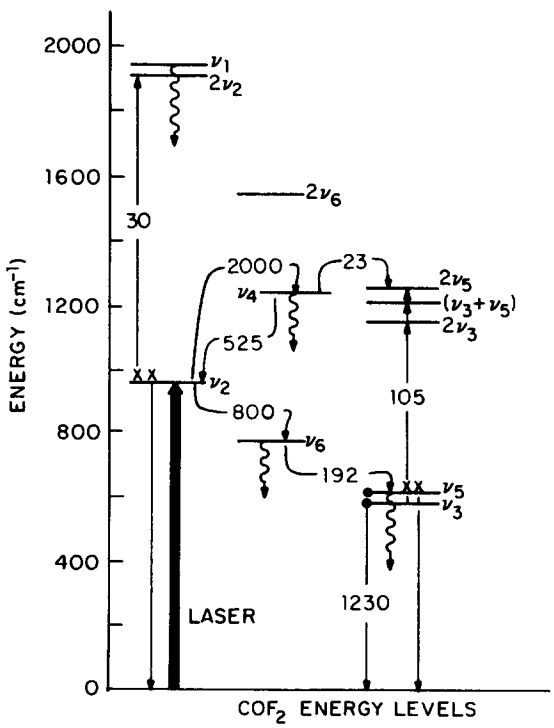

FIG. 3. The dominant vibrational energy transfer pathways in COF_2 and their associated rate constants in units of gas kinetic collisions. A collision diameter of 6 A and a temperature of 296 K were used to convert energy transfer rates to probabilities.

TABLE VII. Probability of vibrational–vibrational energy transfer for COF_2, OCS, SO_2, N_2O, and CO_2.

Species	ΔE[b]	Collision number[a]
COF_2 $(\nu_4 \rightarrow \nu_2)$	280	525[d]
COF_2 $(\nu_2 \rightarrow \nu_6)$	188	800[d]
COF_2 $(\nu_6 \rightarrow \nu_3)$	192/155	190[d]
SO_2 $(\nu_1 \rightarrow 2\nu_2/\nu_2/\nu_0)$	120/640/1151	1600[e]
SO_2 $(\nu_3 \rightarrow \nu_1)$	210	175[e]
OCS $(\nu_1 \rightarrow 2\nu_2)$	−188	2000[f]
OCS $(4\nu_2 \rightarrow \nu_3)$	43	680[f]
N_2O $(\nu_1 \rightarrow 2\nu_2)$	119	400[g]
N_2O $(\nu_3 \rightarrow ?\ 3\nu_2/4\nu_2)$	(−)150 − (+)480 ?	11 000–12 000[c,h]
CO_2 $(2\nu_2 \rightarrow \nu_1)$	−103	< 8[c,i]
CO_2 $(\nu_3 \rightarrow ?)$	(−) 199 − (+)417 ?	25 000[c,j]

[a]Collision numbers are the reciprocals of probabilities.
[b]A positive ΔE (cm^{-1}) denotes an exothermic process.
[c]Collision number was determined directly from the experimentally determined eigenvalue.
[d]This work.
[e]See Refs. 2 and 21.
[f]See Refs. 1 and 18.
[g]See Refs. 22–24.
[h]See Refs. 25 and 26.
[i]See Ref. 22.
[j]See Refs. 27–29.

at a rate corresponding to 2000 gas kinetic collisions.
(b) The ν_6 state is pumped via an exothermic reaction

$$COF_2(\nu_2) + COF_2 \rightarrow COF_2(\nu_6) + COF_2 + 188\ cm^{-1}$$

at a rate corresponding to 800 gas kinetic collisions.

(3) The ν_4 state is rapidly coupled to the overtone states $2\nu_3$, $2\nu_5$ and $(\nu_3+\nu_5)$ in about 25 collisions by near resonant processes such as:

$$COF_2(\nu_4) + COF_2 \rightarrow COF_2(2\nu_3,\ 2\nu_5,\ \nu_3+\nu_5) + COF_2\ .$$

These overtone states rapidly decay to the fundamental states ν_3 and ν_5 by near resonant down-the-ladder collisional processes in approximately 100 collisions.

(4) Population in the ν_6 state is coupled to the ν_3 and ν_5 states at a rate corresponding to 190 gas kinetic collisions via the process

$$COF_2(\nu_6) + COF_2 \rightarrow COF_2(\nu_3,\ \nu_5) + COF_2\ .$$

(5) On a longer time scale, the vibrational state population is lost through V–T,R relaxation of the lowest lying vibrational state

$$COF_2(\nu_3, \nu_5) + COF_2 \rightarrow COF_2 + COF_2$$

at a rate corresponding to 1200 gas kinetic collisions.

The energy transfer probabilities between an out-of-plane mode (ν_6) and the in-plane modes ν_2 and $\nu_{3,5}$ were found to be of the same order of magnitude as typical energy transfer processes involving only in-plane modes. The mixing of the ν_4 state and the overtone states $2\nu_3$, $2\nu_5$, and $\nu_3+\nu_5$ may enhance the rate of energy transfer between ν_4 and the other modes of the molecule, in particular ν_2.

[1]M. L. Mandich and G. W. Flynn, J. Chem. Phys. 73, 1265 (1980).
[2]D. Siebert and G. Flynn, J. Chem. Phys. 62, 1212 (1975).
[3]K. H. Casleton and G. W. Flynn, J. Chem. Phys. 67, 3133 (1977).
[4]R. K. Bohn, K. H. Casleton, Y. V. C. Rao, and G. W. Flynn, J. Phys. Chem. 86, 736 (1982).
[5]P. D. Mallinson, D. C. McKean, J. H. Holloway, and I. A. Oxton, Spectrochim. Acta Part A 31, 143 (1975).
[6]R. S. Sheorey and G. W. Flynn, J. Chem. Phys. 72, 1175 (1980).
[7]G. W. Flynn, Acc. Chem. Res. 14, 334 (1981); E. Weitz and G. Flynn, Adv. Chem. Phys. 47, 185 (1981).
[8]R. D. Bates, J. T. Knudtson, G. W. Flynn, and A. M. Ronn, J. Chem. Phys. 57, 4174 (1972).
[9]E. W. Montroll and K. E. Shuler, J. Chem. Phys. 26, 454 (1957).
[10]R. N. Schwartz, Z. I. Slawsky, and K. F. Herzfeld, J. Chem. Phys. 20, 1591 (1952).
[11]J. L. Stretton, Trans. Faraday Soc. 61, 1053 (1965).
[12]F. I. Tanczos, J. Chem. Phys. 25, 439 (1956).
[13]Y. Yonezawa and T. Funeo, Bull. Chem. Soc. Jpn. 47, 1894 (1974).
[14]E. B. Wilson, Jr., J. C. Decius, and P. C. Cross, *Molecular Vibrations* (McGraw–Hill, New York, 1955).
[15]D. Rapp and T. E. Sharp, J. Chem. Phys. 38, 2641 (1963).
[16]J. C. McCoubrey, R. C. Milward, and A. R. Ubbelohde, Proc. R. Soc. London Ser. A 264, 299 (1961).
[17]J. D. Lambert and R. Salter, Proc. R. Soc. London Ser. A 243, 78 (1957).
[18]M. L. Mandich and G. W. Flynn, J. Chem. Phys. 73, 3679 (1980).
[19]R. L. Taylor and S. Bitterman, Rev. Mod. Phys. 41, 26 (1969).
[20]T. L. Cottrell and J. C. McCoubrey, *Molecular Energy Transfer in Gases* (Butterworths, London, 1961).
[21]J. L. Ahl and G. W. Flynn (to be published).
[22]C. K. Rhodes, M. J. Kelly, and A. Javan, J. Chem. Phys. 48, 5730 (1968).
[23]R. K. Huddleston and E. Weitz, J. Chem. Phys. 74, 2879 (1981).
[24]R. T. V. Kung, J. Chem. Phys. 63, 5305 (1975).
[25]J. T. Yardley, J. Chem. Phys. 49, 2816 (1968).
[26]R. D. Bates, G. W. Flynn, and A. M. Ronn, J. Chem. Phys. 49, 1432 (1968).
[27]F. LePoutre, Ph. D. thesis, Universite de Paris-Sud, Center D'Orsay, March, 1979.
[28]C. B. Moore, R. E. Wood, B. L. Hu, and J. T. Yardley, J. Chem. Phys. 46, 4222 (1967).
[29]L. O. Hocker, M. A. Kovacs, C. K. Rhodes, G. W. Flynn, and A. Javan, Phys. Rev. Lett. 17, 233 (1966).
[30]R. C. Slater and G. W. Flynn, J. Chem. Phys. 65, 425 (1976).